

Cooper pair splitting efficiency in the hybrid three-terminal quantum dot

Grzegorz Michałek · Tadeusz Domański ·
Karol I. Wysokiński

Received: date March 8, 2022/ Accepted: date

Abstract Nanodevices consisting of a quantum dot tunnel coupled to one superconducting and two normal electrodes may serve as a source of entangled electrons. As a result of crossed Andreev reflection the Cooper pair of s-wave character may be split into two electrons and each of them goes into a distinct normal electrode, preserving entanglement. Efficiency of the process depends on the specific system and is tunable by electric means. Our calculations show that in the studied device this efficiency may attain values as large as 80%.

Keywords Cooper pair splitting · hybrid structures · Andreev reflection

PACS 73.23.-b · 73.63.Kv · 74.45.+c

1 Introduction

One of the important motivations to study hybrid many-terminal nanostructures with normal and superconducting leads is a perspective to obtain the non-locally entangled electrons [1]. Electrons of s-wave superconductors are known to exist in the spin singlet, maximally entangled states. When two electrons forming such Cooper pair are split (on interface between superconductor and other materials), they still preserve entanglement albeit being spatially separated. Splitting mechanism can be achieved [2,3] by the Andreev

This work is partially supported by the National Science Centre in Poland via the project DEC-2014/13/B/ST3/04451.

G. Michałek
Institute of Molecular Physics, Polish Academy of Sciences, 60-179 Poznań, Poland
T. Domański, K. I. Wysokiński
Institute of Physics, M. Curie-Skłodowska University, 20-031 Lublin, Poland
Tel.: +48-81 537 6236
Fax: +48-81 537 6190
E-mail: karol.wysokinski@poczta.umcs.lublin.pl

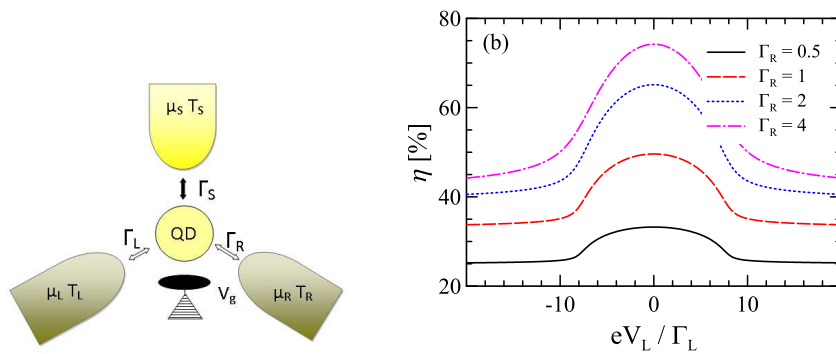


Fig. 1 (a) Sketch of the system. (b) Efficiency η with respect to V_L for $\Gamma_S/\Gamma_L = 16$, $\epsilon_0 = 0$, $U = 0$, $V_R = 0$, $T = 0$ and $\Gamma_R/\Gamma_L = \{0.5, 1, 2, 4\}$. Γ_L is treated as unity in our calculations.

scattering processes. In many-terminal hybrid device with one superconducting electrode (Fig. 1a) the crossed Andreev reflection (CAR) occurs when one of the electrons enters, say left (L) electrode while its partner goes to the right (R) one. The Cooper pair splitting (CPS) in such Y-shape junctions has been proposed theoretically [2, 3, 4] and realised experimentally by several groups [5, 6, 7, 8, 9, 10, 11].

It has been suggested that the highest efficiency of CPS can be achieved in three-terminal hybrid devices using the double quantum dots with strong intradot Coulomb repulsion [3]. We have previously analysed the Y-shape junction with only a single quantum dot [12], where interplay between the local and non-local processes is controlled by suitable choice of the quantum dot level, the couplings and applied voltages [13]. The analysis of the thermoelectric properties [14, 15] of this three terminal hybrid system has shown that Seebeck coefficient can be large, but the symmetry of the model prevents a direct contribution of the CAR to both the local and non-local thermopower [15].

Regions in the parameter space, where CAR processes are dominant under realistic experimental conditions [12, 13, 15] are expected to be also useful for the efficient CPS. It is the aim of this work to quantify such conjecture by calculating CPS efficiency as defined in Eq. (6) below. The paper is organised as follows. In section 2 we introduce the model, discuss the approach and define the CPS efficiency. Our results are presented in section 3 and in section 4 we end with the brief summary.

2 The system, its modelling and efficiency of CPS

We consider the system, consisting of a quantum dot (QD) coupled to two normal (left - L and right - R) electrodes and another superconducting (S) lead. Such heterostructure (Fig. 1a) can be modelled by the Hamiltonian

$$H = H_{QD} + \sum_{\alpha=L,R,S} H_{\alpha} + H_T, \quad (1)$$

where H_{QD} describes the quantum dot, H_α refers to electrons of α -th lead and H_T is a hybridisation between the leads and the QD. Various parts of the Hamiltonian read $H_{QD} = \epsilon_0 \sum_\sigma d_\sigma^\dagger d_\sigma + U n_\uparrow n_\downarrow$, where ϵ_0 is the single-particle energy level, d_σ^\dagger (d_σ) denotes creation (annihilation) operator of the dot electron with spin σ , $n_\sigma \equiv d_\sigma^\dagger d_\sigma$ is the number operator, and U is the repulsive Coulomb interaction. The normal metal electrodes are treated within the mean field approximation $H_\alpha = \sum_{k,\sigma} \epsilon_{\alpha k} c_{\alpha k \sigma}^\dagger c_{\alpha k \sigma}$, where $c_{\alpha k \sigma}^\dagger$ ($c_{\alpha k \sigma}$) denotes creation (annihilation) of an electron with spin σ and momentum k in the electrode $\alpha = \{L, R\}$. The superconducting electrode is described in the BCS approximation by $H_S = \sum_{k,\sigma} \epsilon_{S k} c_{S k \sigma}^\dagger c_{S k \sigma} + \sum_k \left(\Delta c_{S -k \uparrow}^\dagger c_{S k \downarrow}^\dagger + \Delta^* c_{S k \downarrow} c_{S -k \uparrow} \right)$, where we have assumed the isotropic energy gap Δ . Coupling between the QD and the external leads is given by $H_T = \sum_{\alpha,k,\sigma} \left(V_{\alpha,k} c_{\alpha k \sigma}^\dagger d_\sigma + V_{\alpha,k}^* d_\sigma^\dagger c_{\alpha k \sigma} \right)$, where $V_{\alpha,k}$ describes the hopping of an electron between QD and the state k in the α lead. Electron and hole transfer between the QD and the leads is described by an effective tunneling rate Γ_α , which in the wide-band approximation takes the form $\Gamma_\alpha = 2\pi \sum_k |V_{\alpha,k}|^2 \delta(E - \epsilon_{\alpha k})$ and is assumed to be energy independent. We shall consider finite voltage V_L applied to the left electrode, whereas the superconducting and right electrodes are grounded.

In this work we are predominantly interested in the CPS, therefore we assume that the voltage $|V_L|$ is safely smaller than the superconducting gap. Focusing on the subgap transport we determine the current I_α^{TOT} flowing from the normal α electrode [16,17]

$$I_\alpha^{TOT} = I_\alpha^{ET} + I_\alpha^{AR} = I_\alpha^{ET} + I_\alpha^{DAR} + I_\alpha^{CAR}, \quad (2)$$

where

$$I_\alpha^{ET} = \frac{2e}{h} \Gamma_\alpha \Gamma_{\tilde{\alpha}} \int |G_{11}^r(E)|^2 [f_\alpha(E) - f_{\tilde{\alpha}}(E)] dE, \quad (3)$$

$$I_\alpha^{DAR} = \frac{2e}{h} \Gamma_\alpha^2 \int |G_{12}^r(E)|^2 [f_\alpha(E) - \tilde{f}_\alpha(E)] dE, \quad (4)$$

$$I_\alpha^{CAR} = \frac{2e}{h} \Gamma_\alpha \Gamma_{\tilde{\alpha}} \int |G_{12}^r(E)|^2 [f_\alpha(E) - \tilde{f}_{\tilde{\alpha}}(E)] dE. \quad (5)$$

Here $\tilde{\alpha}$ denotes normal electrode different from α while $f_\alpha(E) = \{\exp[(E - eV_\alpha)/k_B T_\alpha] + 1\}^{-1}$ and $\tilde{f}_\alpha(E) = 1 - f_\alpha(-E) = \{\exp[(E + eV_\alpha)/k_B T_\alpha] + 1\}^{-1}$ are the Fermi-Dirac distribution functions in the electrode $\alpha = \{L, R\}$ for electrons and holes, respectively. I_α^{ET} denotes the current contributed by the normal electron transfer (ET) and I_α^{AR} stands for the Andreev reflection (AR) processes due to the direct (DAR) and the crossed (CAR) scatterings. The current flowing from the S-electrode is denoted I_S^{TOT} . The Kirchoff's law $I_L^{TOT} + I_R^{TOT} + I_S^{TOT} = 0$ is fulfilled.

In order to establish the optimal CPS efficiency we guide ourselves by the previous studies [12,13], looking for the model parameters where the CAR processes are dominant. We use the following definition of CPS efficiency

$$\eta = \frac{2|I^{CAR}|}{2|I^{ET}| + |I_L^{DAR}| + |I_R^{DAR}| + 2|I^{CAR}|}, \quad (6)$$

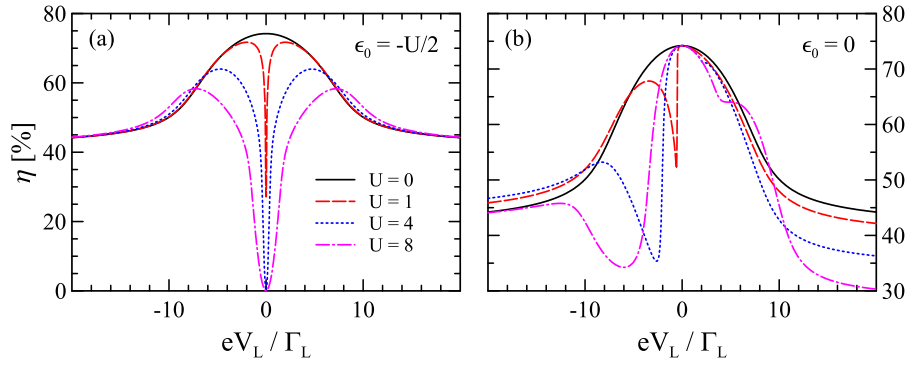


Fig. 2 Dependence of the CPS efficiency η on the voltage V_L for $\Gamma_S/\Gamma_L = 16$, $\Gamma_R/\Gamma_L = 4$, $V_R = 0$, $T = 0$, $U/\Gamma_L = \{0, 1, 4, 8\}$ and (a) $\epsilon_0 = -U/2$, (b) $\epsilon_0 = 0$.

where $I^{CAR} \equiv I_L^{CAR} = I_R^{CAR}$ and $I^{ET} \equiv I_L^{ET} = -I_R^{ET}$. The expression (6) generalises $\eta = 2|I^{CAR}| / (2|I^{CAR}| + |I_L^{DAR}| + |I_R^{DAR}|)$ previously introduced under isothermal conditions for $V_L = V_R \neq V_S$ [6] and is consistent with the definition $\eta = |I^{CAR}| / (|I^{CAR}| + |I^{ET}|)$ used in absence of any electrostatic voltage for $T_L \neq T_R$ [18]. In what follows we investigate the CPS efficiency (6) for producing the entangled electrons as a consequence of competition between the CAR and other transport channels.

3 Results

Figs 1-3 show the results obtained numerically for voltages $V_R = V_S = 0$ and temperature $T = 0$. We have imposed the strong coupling condition to superconducting electrode assuming $\Gamma_S \gg \Gamma_{L,R}$ in order to promote the Andreev processes. For the sake of completeness we start the analysis with a simple noninteracting case $U = 0$. Fig. 1b displays the CPS efficiency η as a function of the voltage V_L applied to the normal L electrode for QD level position $\epsilon_0 = 0$ and for various couplings to the normal R electrode. Magnitude of η depends on Γ_R and its flat maximum occurs for $V_L \rightarrow 0$, where the ET processes are suppressed because of the proximity induced on-dot gap. The CPS efficiency decreases when voltages exceeds the Andreev bound states (at energies $\pm\sqrt{\epsilon_0^2 + \Gamma_S/4}$) which are formed in the QD due to the proximity effect [12]. The increase of η with Γ_R is caused by the CAR processes, dominant over the DAR currents (for $\Gamma_R > 2\Gamma_L$). Let us note, however, that the ET current is also sensitive to Γ_R . This can be seen for large Γ_R (not shown) when the CPS efficiency eventually decreases. Let us emphasize that for other electrical bias configurations (e.g. $V_R = V_L$, $V_R = -V_L$) the CPS efficiency is reduced. For example, $\eta \rightarrow 0$ for $V_R = -V_L$ and $T \rightarrow 0$ due to the strong suppression of the CAR processes.

Fig. 2 presents the CPS efficiency (6) obtained for the correlated quantum dot, where the Coulomb interactions are treated in the Hubbard I approxi-

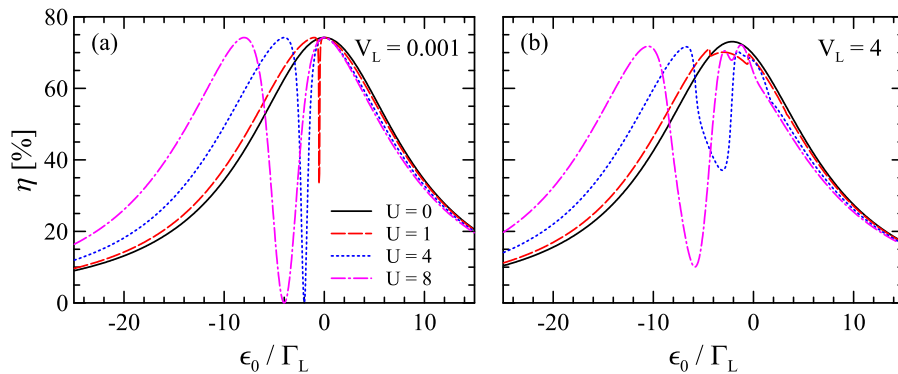


Fig. 3 Efficiency η as a function of the quantum dot level ϵ_0 for (a) small $eV_L/h\Gamma_L = 0.001$ and (b) large $eV_L/h\Gamma_L = 4$. The other parameters are the same as in Fig. 2.

mation (*e.g.* [19,12]). For finite U , in contrast to the noninteracting case, four Andreev bound states [12] appear in the density of states of the QD. For the electron-hole symmetric case $\epsilon_0 = -U/2$ the CPS efficiency η is a symmetric function of the applied bias voltage V_L . The CPS efficiency diminishes with an increasing Coulomb repulsion. For small voltages, when system is in the Coulomb blockade regime (*i.e.* in the region between the inner Andreev bound states) there appears a dip, where η is reduced. It is in contrast with the noninteracting case where the maximum of η appeared between Andreev bound states. This behaviour is manifestation of the Coulomb blockade effect, which suppresses the CAR processes more efficiently than the ET processes [13]. As the separation of the Andreev bound states grows with an increase of the electron interactions U the corresponding distance between maxima of the CPS efficiency also increases. When the electron-hole symmetry is broken (*e.g.* for $\epsilon_0 = 0$) we can notice that the CPS efficiency characteristics are asymmetric with respect to the $V_L = 0$. This behavior is caused by the ET contribution, which amplitude is sensitive on the position of the ϵ_0 . We can also observe a dip, which is less pronounced and slightly shifted to larger voltages $|V_L|$ while the magnitude and position of the maximum remains unchanged.

Variation of the CPS efficiency η with respect to the quantum dot level ϵ_0 is shown in Fig. 3. For small bias $V_L/\Gamma_L = 0.001$ the optimal values of η appear symmetrically with respect to the particle-hole symmetry point $\epsilon_0 \simeq -U/2$ where η vanishes. The height of both peaks remain unchanged by the Coulomb potential, in analogy to the recent observation of CPS in the Josephson junction[20]. For larger bias $V_L/\Gamma_L = 4$ the situation is a bit more complicated as the pronounced dip between the peaks appears for sufficiently large electron-electron interactions. Position of the maxima are slightly shifted relative to the small bias case. The optimal CPS efficiency can be precisely tuned by the gate voltage which shifts the energy level ϵ_0 and by the bias voltage V_L . This complex behaviour of η is driven by a competition between the ET, DAR and CAR processes in accord with earlier discussion [12].

4 Summary

We have extended our previous studies [12,13,15] by analysing the efficiency of the Cooper pair splitting in a hybrid system, consisting of the quantum dot coupled to one superconducting and two metallic electrodes. We have found that the CPS efficiency is tunable (by changing the system parameters) and its optimal value can approach nearly 80%. The repulsive interactions have the destructive influence on such efficiency. In the Coulomb blockade regime the CPS efficiency is suppressed due to the reduced probability to find a pair of electrons on the quantum dot.

In distinction to Ref. [18] (corresponding to the Y-shape heterostructure with two quantum dots) we have found that our system does not allow for any non-zero CPS efficiency originating solely from the temperature difference (i.e. in absence of any external voltage). This effect is caused by the particle-hole symmetry of the crossed Andreev reflections, as has been recently emphasized in a context on the thermoelectric properties [15].

References

1. R. Horodecki, P. Horodecki, M. Horodecki, and K. Horodecki, *Rev. Mod. Phys.* **81**, 865 (2009).
2. J. Torr es and T. Martin, *Eur. Phys. J. B* **12**, 319 (1999).
3. P. Recher, E. V. Sukhorukov, and D. Loss, *Phys. Rev. B* **63**, 165314 (2001).
4. N. M. Chtchelkatchev, G. Blatter, G. B. Lesovik, and T. Martin, *Phys. Rev. B* **66**, 161320(R) (2002).
5. L. Hofstetter, S. Csonka, J. Nyg ard, and C. Sch onenberger, *Nature* **461**, 960 (2009).
6. L. G. Herrmann, F. Portier, P. Roche, A. L. Yeyati, T. Kontos, and C. Strunk, *Phys. Rev. Lett.* **104**, 026801 (2010).
7. J. Wei and V. Chandrasekhar, *Nat. Phys.* **6**, 494 (2010).
8. L. Hofstetter, S. Csonka, A. Baumgartner, G. F ul op, S. d'Hollosy, J. Nyg ard, and C. Sch onenberger, *Phys. Rev. Lett.* **107**, 136801 (2011).
9. J. Schindele, A. Baumgartner, and C. Sch onenberger, *Phys. Rev. Lett.* **109**, 157002 (2012).
10. A. Das, Y. Ronen, M. Heiblum, D. Mahalu, A. V. Kretinin, and H. Shtrikman, *Nat. Commun.* **3**, 1165 (2012).
11. J. Schindele, A. Baumgartner, R. Maurand, M. Weiss, and C. Sch onenberger, *Phys. Rev. B* **89**, 045422 (2014).
12. G. Michałek, B. R. Bułka, T. Domański, and K. I. Wysokiński, *Phys. Rev. B* **88**, 155425 (2013).
13. G. Michałek, T. Domański, B. R. Bułka, and K. I. Wysokiński, *Sci. Rep.* **5**, 14572 (2015).
14. K. I. Wysokiński, *J. Phys.: Condens. Matter* **24**, 335303 (2012).
15. G. Michałek, M. Urbaniak, B. R. Bułka, T. Domański, and K. I. Wysokiński *Phys. Rev. B* **93**, 235440 (2016).
16. C. Niu, D. L. Lin, and T.-H. Lin, *J. Phys.: Condens. Matter* **11**, 1511 (1999).
17. Q.-F. Sun, J. Wang, and T.-H. Lin, *Phys. Rev. B* **59**, 3831 (1999); *Phys. Rev. B* **62**, 648 (2000); Y. Zhu, T.-H. Lin, and Q.-F. Sun, *Phys. Rev. B* **69**, 121302 (2004).
18. Z. Cao, T. F. Fang, L. Li, and H. G. Luo, *Appl. Phys. Lett.* **107**, 212601 (2015).
19. H. Haug and A.-P. Jauho, *Quantum Kinetics in Transport and Optics of Semiconductors, Second, Substantially Revised Edition*, Springer Verlag, Berlin (2008).
20. R. S. Deacon, A. Oiwa, J. Sailer, S. Baba, Y. Kanai, K. Shibata, K. Hirakawa, and S. Tarucha, *Nat. Commun.* **6**, 7446 (2015).